Eur Biophys J (2006) 35: 125–135
DOI 10.1007/s00249-005-0026-6

REVIEW

Susana Pereira · Nuno M.F.S.A. Cerqueira
Pedro Alexandrino Fernandes · Maria João Ramos

Computational studies on class I ribonucleotide reductase: understanding the mechanisms of action and inhibition of a cornerstone enzyme for the treatment of cancer

Received: 21 May 2005 / Revised: 21 September 2005 / Accepted: 28 September 2005 / Published online: 29 October 2005

Abstract This review provides a synthesis of recent work, using computational methods, on the action and inhibition mechanisms of class I ribonucleotide reductase (RNR). This enzyme catalyzes the rate-limiting step of the pathway for the synthesis of DNA monomers and, therefore, has long been regarded as an important target for therapies aiming to control pathologies that depend strongly on DNA replication. In fact, over the last years, several molecules, which are able to impair RNR activity by different mechanisms, have been applied effectively in anti-cancer, anti-viral and anti-parasite therapies. A better understanding of the chemical mechanisms involved in normal catalysis and in inhibition of the enzyme is important for the rational design of more specific and effective inhibitor compounds. To achieve this goal, computational methods, particularly quantum chemical calculations, have been used more and more frequently. The ever-growing capabilities of these methods together with undeniable advantages make it a stimulating area for research purposes.

Introduction

Ribonucleotide reductase (RNR) catalyzes the conversion of ribonucleotides into the correspondent 2′-deoxyribonucleotides, in the rate limiting step for the biosynthesis of DNA (Reichard 1993; Stubbe and van der Donk 1998).

Ribonucleotide reductase is a ubiquitous radical-containing enzyme, which is usually classified into three different types, according to the cofactor needed to produce the essential organic radical, the active site residues that perform catalysis, and the phosphorylation state of the substrates. The *Escherichia coli* RNR is similar to the mammalian one (class I) and has served as its prototype in experimental and computational studies; these were much facilitated by the determination of the R1 and R2 subunits' X-ray crystallographic structure (Eriksson et al. 1997; Nordlund et al. 1990; Uhlin and Eklund 1994).

Escherichia coli RNR is an $\alpha_2\beta_2$ tetramer that results from the association of two catalytically inactive homodimers, R1 (α_2) and R2 (β_2) (see Fig. 1). Subunit R2 is the smaller of the two, with a molecular weight of 87 kDa, and contains a non-heme di-iron cluster, which is involved in generating and stabilizing the radical essential for catalysis. This radical is located in a tyrosine residue (Tyr_{122}), it is formed upon dissociation of a molecule of O_2 by the binuclear ferrous [Fe(II)] complex, and is stabilized by the resulting oxo-bridged ferric [Fe(III)] dimer (see Fig. 2). The active site of the enzyme and the allosteric sites that regulate its specificity and activity are all located in the bigger R1 subunit, which has a molecular weight of 171 kDa. When the substrate (a ribonucleoside-5′-diphosphate) binds to the active site, in R1, the radical character has to be transferred from the Tyr_{122} in R2 to a cysteine residue (Cys_{439}) of the active site, which will in turn initiate the catalytic reaction. These two amino acid residues are ca. 35 Å apart and the radical character relocation is believed to occur via hydrogen atom transfers along a pathway of conserved hydrogen-bonded residues. As for the catalysis itself, the active site residues directly involved in the set of reactions are three cysteines (Cys_{439}, Cys_{225} and Cys_{462}), one glutamate (Glu_{441}) (Persson et al. 1997) and one asparagine (Asn_{437}) (Kasrayan et al. 2002) (see Fig. 3). The reduction of the substrate leads to elimination of a water molecule and oxidation of Cys_{225} and Cys_{462} to a disulfide bridge (Stubbe and van der Donk 1998).

The same enzyme is responsible for the reduction of all four ribonucleotides. Its specificity towards each

S. Pereira · N.M.F.S.A. Cerqueira · P. A. Fernandes
M. J. Ramos (✉)
REQUIMTE/Departamento de Química,
Faculdade de Ciências do Porto, Rua do Campo Alegre, 687,
4169-007 Porto, Portugal
E-mail: pafernan@fc.up.pt

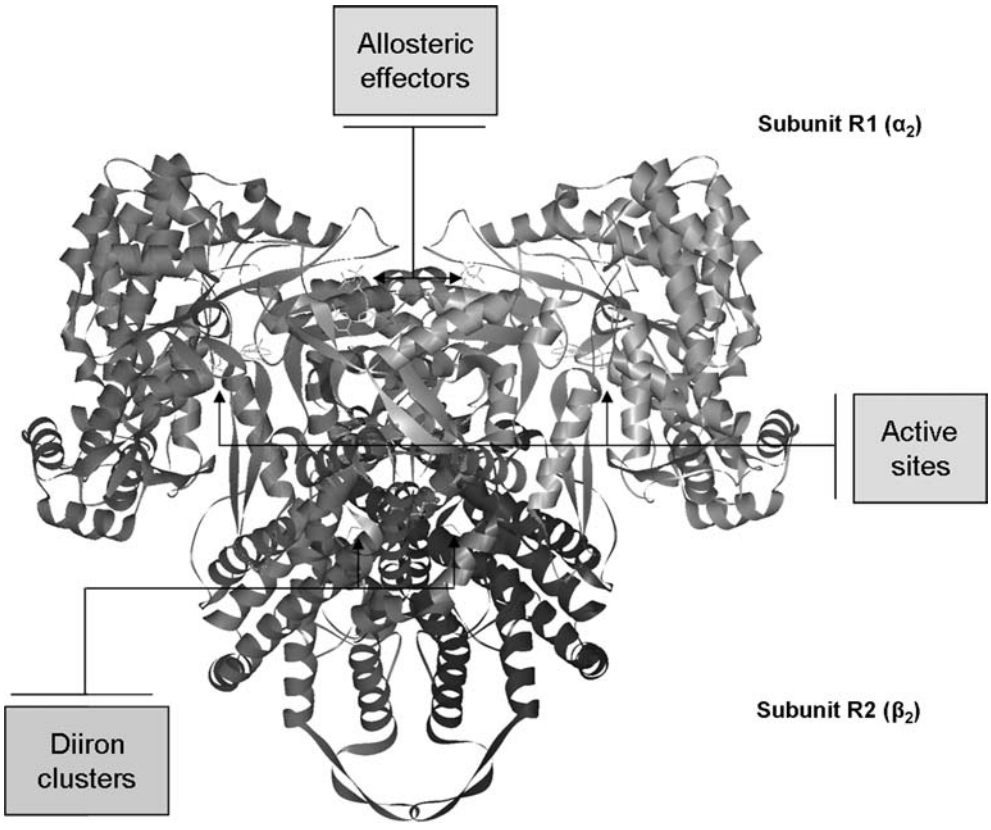

Fig. 1 X-ray crystallographic structure of *E. coli* RNR in ribbon representation

substrate depends on the actual needs of the cell and is controlled by the interaction of the right nucleotide effector with an allosteric site of RNR. Its general activity is also regulated allosterically and is cell cycle-dependent. These regulation mechanisms ensure the permanent maintenance of a low cellular pool of deoxyribonucleotides, and make DNA replication and repair greatly dependent on the performance of RNR. Naturally, these features have long made RNR a key target for therapies aiming to attack or control proliferation-based diseases.

The RNR inhibitors hydroxyurea and gemcitabine are presently being used in the clinical treatment of melanoma, resistant chronic myelocytic leukaemia, carcinoma of the ovary, non-small cell lung cancer, pancreatic cancer, breast cancer and bladder cancer (http://www.fda.gov). Moreover, a growing number of clinical trials are being carried with these and other RNR inhibitors assessing their efficacy in different therapies, including anti-cancer, anti-viral and anti-parasite (Balzarini 2000; Ingram and Kinnaird 1999; Johns and Gao 1998; Manegold 2004; Romanelli et al. 1999; Tripathy 2002; Tsimberidou et al. 2002).

Ribonucleotide reductase inactivation may be achieved in numerous ways (Cerqueira et al. 2005). It can be induced, for instance, in an earlier phase, by interfering with the synthesis of the enzyme subunits or by preventing their interaction—using mRNA complementary nucleotide sequences, or small peptides that mimic the sequence responsible for the subunits' interaction. When the enzyme is in its active form, inhibition can be brought about with radical scavengers that interact with subunit R2 and destroy the essential tyrosyl radical—this is the inhibition mechanism of hydroxyurea. Another group of inhibitors that interact with the enzyme in its functional state consists of nucleoside-triphosphate and nucleoside-diphosphate analogs. The former interacts with the binding sites for the allosteric effectors (Harrington and Spector 1991); the latter, known as suicide inhibitors, are recognized by RNR as normal substrates and react with the active site leading to abnormal products that alkylate the protein and turn it enzymatically inactive—gemcitabine is an example of this latter group of molecules (see Fig. 4).

A comprehensive knowledge and thorough understanding of every process involved in the normal RNR functioning and in its inhibition mechanisms is very important to design new compounds, sought to inhibit the enzyme in a more specific and effective manner. To this end, computational methods, and particularly quantum chemical calculations, are an indispensable complement to structural biology studies and biochemical experiments. One advantage is that they can provide structural information on transition states and snapshots of molecules in the act of reaction; direct detection of such transient events is not possible by normal physical methods. This is particularly important in the case of RNR, where radical species are involved. Moreover, computational studies enable the identification of unstable intermediates, and thus the elucidation

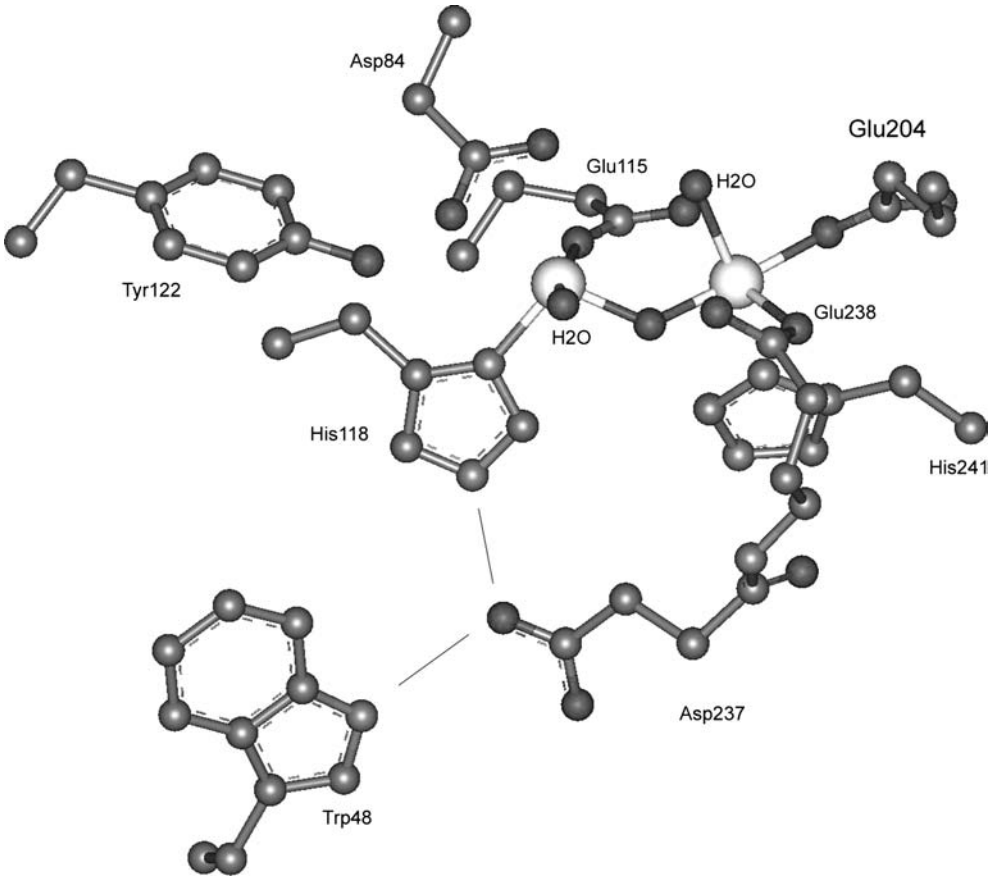

Fig. 2 *E. coli* RNR di-iron cluster X-ray crystallographic structure in its oxidized form (Nordlund and Eklund 1993). The residues co-ordinating the iron atoms are shown, as well as the tyrosine residue where the organic radical is first generated (Tyr_{122}), and also the first elements of the hydrogen-bonded chain that carry the radical character between Tyr_{122} and Cys_{439} in the active site, that is, Hys_{118}, Asp_{237} and Trp_{48}

of the chemical mechanisms involved in these processes, with atomic detail.

In the following four sections, we will review recent mechanistic studies that were performed with quantum chemical calculations, focusing specifically on the following aspects of RNR chemistry: di-iron cluster and tyrosyl radical formation; radical character transfer to the active site; catalytic mechanism; and inhibition mechanism by substrate analogs. The aim of these studies is to support the large efforts that are being made by the scientific and pharmaceutical communities in terms of the rational drug design for anti-cancer therapy. As the most promising inhibitors for clinical use are mechanism-based ones, a deep knowledge about the involved mechanisms is urgently needed if one wants to proceed rationally towards new drugs that are more potent, more specific and less toxic than the ones currently in use.

Di-iron cluster and tyrosyl radical generation

The di-iron cluster of RNR, in its reduced form, is composed of two ferrous iron atoms co-ordinated to two histidine residues and four carboxylate groups (three glutamate and one aspartate side chains). The iron dimer is oxidized by a direct reaction with an oxygen molecule: one oxygen atom is reduced to H_2O, and the other is incorporated as a bridging oxo in the diferric complex (see Fig. 2); the reaction also results in a radical tyrosine residue (Tyr_{122}). Several intermediates of this process have been observed, namely by Mössbauer and resonance Raman spectroscopies—the iron spins of these complexes are usually anti-ferromagnetically coupled, which means that the ones with an even number of electrons are invisible by EPR. One of these intermediates is a compound termed **P**, which has been suggested to be an $[Fe(III)]_2$ peroxo complex, although so far it has only been detected in R2 variants (e.g., R2-D84E). Another compound, termed **X**, is the intermediate with the highest oxidation state observed, and has been spectroscopically characterized as an Fe(IV)Fe(III) dimer (Sturgeon et al. 1996). After **X** is formed, the next step is the abstraction of a proton and an electron from Tyr_{122}, thus forming the catalytic essential tyrosyl radical (Bollinger et al. 1994). As this radical is formed, the iron dimer is reduced to the resting oxo-bridged diferric state. To gain insight into the details of these complex processes quantum-chemical calculations have been widely used (Torrent et al. 2002; Noodleman et al. 2004; Himo and Siegbahn 2003); they will be now briefly discussed.

To assign possible structures for the observed intermediates, Siegbahn carried a theoretical study with a model of the iron dimer complex, which included the first ligand sphere represented by four carboxylates and two imidazoles (Siegbahn 1999). The experimental X-ray

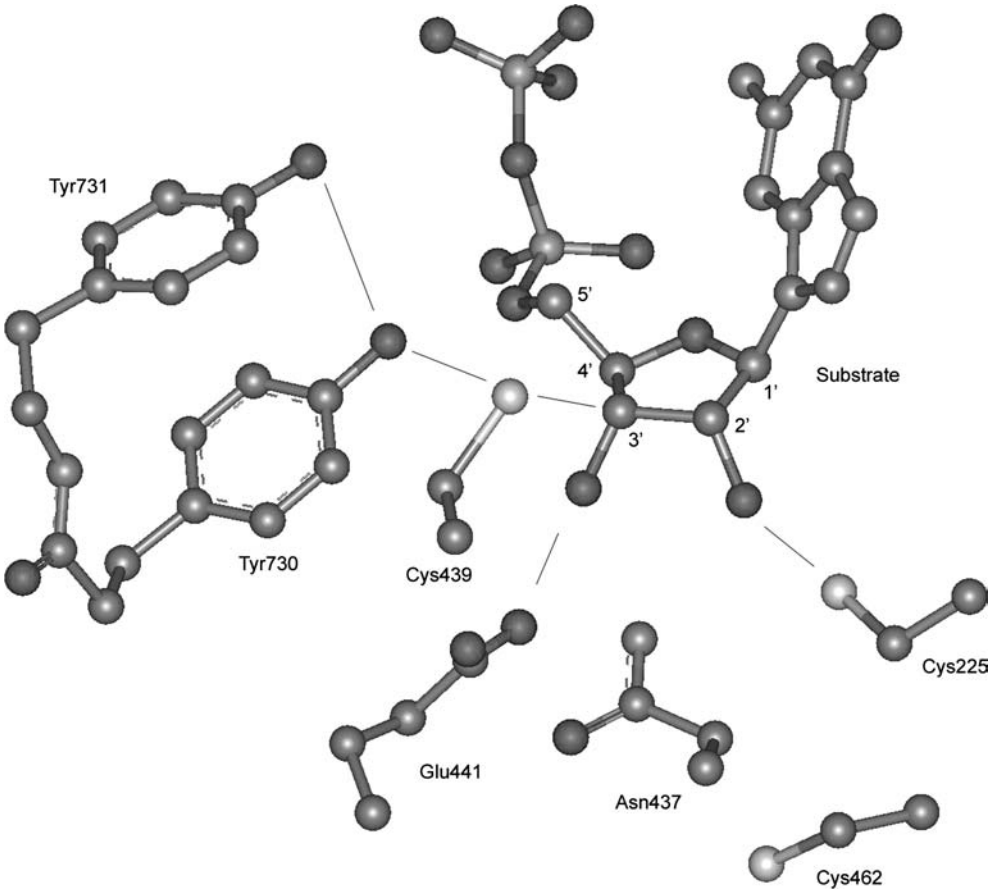

Fig. 3 Active-site X-ray crystallographic structure of *E. coli* RNR with bound substrate (Eriksson et al. 1997). For simplicity, only the side chains of the residues are showed; the main hydrogen bonds are indicated by *lines*; Tyr_{730} and Tyr_{731} are believed to be the two final amino acid residues of the hydrogen-bonded chain that transports the radical character to Cys_{439}

structure (Nordlund et al. 1990) was used as a starting point for the optimization of the resting diferric state; it was observed that its main features, concerning bond directions and rough bond distances, were well reproduced by the calculations. Possible structures for compounds **P** and **X** were searched, always taking into account the data obtained from experimental studies, and assuming that the complexes should be maintained

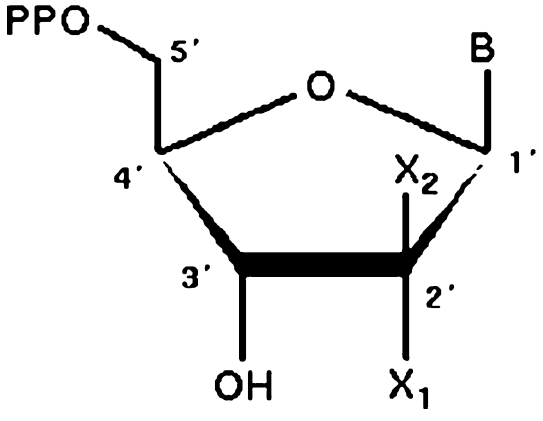

Fig. 4 Structure of the RNR substrate, product and some suicide inhibitors: $X_1 = OH$; $X_2 = H$: RNR substrate; $X_1 = X_2 = H$: product of RNR catalysis; $X_1 = X_2 = F$: Gemcitabine; $X_1 = Cl$, F, N_3; $X_2 = H$: other examples of suicide inhibitors

neutral (because the iron cluster is buried in the low dielectric medium of the protein, where charge build-up will not easily occur). For intermediate **P**, two possible structures were optimized, which differed mainly in the position of the oxygen molecule relative to the iron atoms; based on experimental information, the one with the peroxo group symmetrically placed between them was chosen as the best candidate for the compound. A structure for intermediate **X** was also suggested, which is consistent with bond distance information obtained from experimental studies, but is quite different from the experimentally deduced proposal; the main difference is the existence of a hydroxyl group bridging the iron atoms in addition to the oxo-bridge that was proposed to be the only one by experimentalists.

The structure of compound **X**, and particularly whether or not the iron atoms have two oxo-bridges derived from the oxygen molecule, was also investigated theoretically by Han et al. (2003). The initial calculations were performed on a small model cluster that included first-shell ligands derived from the amino acid side chains. These first calculations showed that the introduction of the second oxygen species is most energetically favored as a bridging hydroxide. To incorporate second-shell hydrogen bonding as well as possible charge-transfer effects to the cluster, the most favored small model, which contained the oxo- and the

hydroxide bridges, was surrounded by second- and third-shell H-bonding partners similar to those found in the RNR protein environment for the resting and reduced oxidation states. The analysis of the model's calculated properties, however, revealed inconsistencies with known experimental ones, particularly with the Mössbauer data, which implied that the structure under consideration was not likely to be the mysterious compound **X**.

The same group undertook similar procedures to investigate the plausibility of another proposal for compound **X** (Han et al. 2004). This hypothesis had been suggested by Burdi et al. (1998) based on new experimental results; the proposed structure contained the two oxygen atoms initially derived from oxygen—one involved in the oxo bridge, and the other as a terminal aqua ligand bound to the Fe(III) of the Fe(III)Fe(IV) dimer—and one or two additional mono-oxygen bridges provided by carboxylates. Again, the comparison of the calculated properties with the experimental data indicates that the studied models are unlikely to be representative of the core structure of RNR intermediate **X**.

Yang et al. (2000) investigated the geometric and electronic structures of the reduced di-iron cluster both of RNR and of stearoyl acyl carrier protein Δ^9 desaturase and explored the electronic contributions to their different oxygen reactivity. Theoretical calculations were used to describe the electronic structure of the reduced di-iron cluster and to explore its reactivity towards oxygen. The system that was used to represent the RNR di-iron complex was derived from the R2 subunit X-ray crystallographic coordinates (Logan et al. 1996), after adjusting the bond lengths to be within the range found for binuclear ferrous model complexes, and also to agree with complementary spectroscopic studies. After optimization of the geometry, the electronic structure of the complex was characterized and possible ways of oxygen binding were explored. Binding of oxygen to the iron atoms in a bridged mode, with two-electron transfer from the metals to the oxygens, was found to be the more energetically favored mechanism; it involves the rearrangement of the carboxylate ligands and results in direct formation of the $[Fe(III)]_2$ peroxo-bound species (intermediate **P**) (see Fig. 5).

The same type of study was performed by Wei et al. (2004), but in this case, the aim of the spectroscopic/DFT studies was to provide insight into the geometric and electronic differences between the reduced binuclear iron complexes of two R2 variants (R2-D84E and R2-W48F/D84E), the R2-wt and methane mono-oxygenase (MMOH), which is another di-iron cluster-containing enzyme. This knowledge should improve the understanding of their structural differences and help in their correlation to a diverse O_2 reactivity. The di-iron cluster of MMOH is characterized by having two histidine and four glutamate residues coordinating the iron atoms, which means that it differs from the R2 complex only in one residue; in the R2-D84E variant this difference is gone. Nevertheless, the study showed that, although the central ligand set is the same in MMOH and R2-D84E, the protein environment must play a major role in structuring the di-iron complex. In fact, the geometric and electronic structures of the single and double R2-variants were found to be unlike MMOH in co-ordination, geometry and mode of bridging; the closer similarity to wt-R2 could thus be due to the influence of second sphere residues.

It is believed that the carboxylate ligands play a special role in the proper functioning of the metal complex. In fact, the flexibility of these ligands allows them to co-ordinate the iron centers as a function of the enzymatic needs: as bidentate ligands when saturation of the first sphere is required, and as monodentate when one or more vacant co-ordination sites are needed. The issue of the carboxylate ligands flexibility was addressed in a theoretical study by Torrent et al. (2001). In this study, quantum chemical methods were used to investigate two processes: the carboxylate shift that involves the two iron atoms (1,2-carboxylate shift), and the bidentate–monodentate carboxylate rearrangement within the same iron center (see Fig. 6). The different structures were found to be energetically very close and separated by small energetic barriers, which means that both rearrangement processes take place very easily. The calculations are consistent with the available experimental data that showed high flexibility of the carboxylate ligands and a non-rigid core structure.

In summary, although great effort is being made toward the understanding of the di-iron cluster reactivity and the generation of the tyrosyl radical, the overall process still remains elusive, and further studies are needed if one wants to rationally design a new

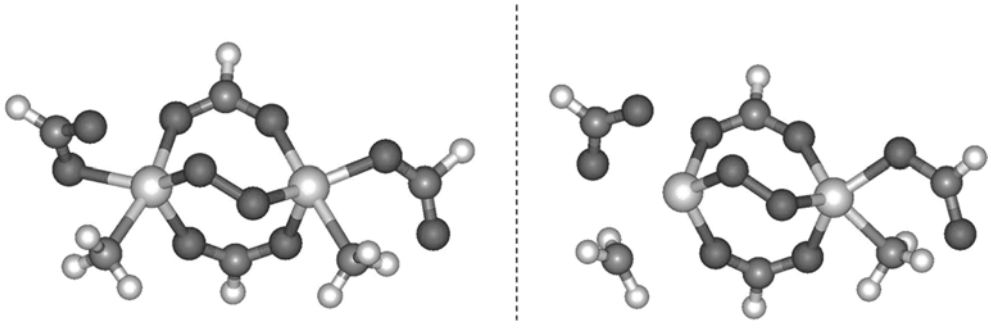

Fig. 5 Energy-minimized structures of the RNR di-iron cluster, with the oxygen molecule bound in a bridged mode, before and after the carboxylate rearrangement (Yang et al. 2000)

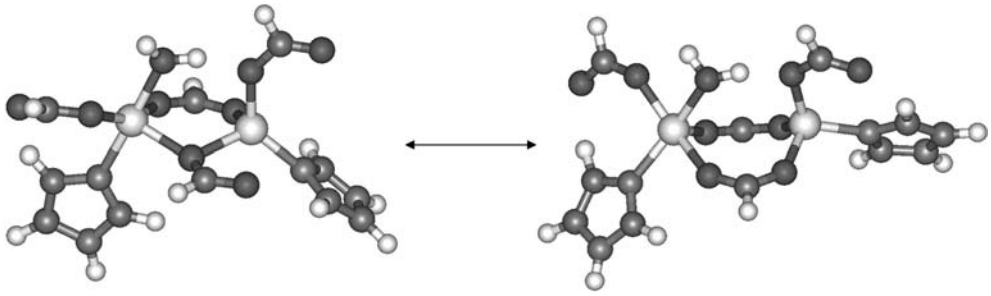

Fig. 6 An illustration of carboxylate flexibility in the first co-ordination sphere of the di-iron cluster (Torrent et al. 2001)

generation of potent, specific R2 radical scavengers to be used in the context of RNR inhibition.

Radical transfer to the active site

The organic free radical essential for RNR catalysis is generated at the amino acid residue Tyr_{122}, which is deeply buried in subunit R2, close to the di-iron cluster. Upon hydrogen bonding of the substrate to the active site, the radical has to be relocated to Cys_{439}, which will effectively start the catalytic reaction, by abstracting an H-atom from the sugar moiety of the ribonucleotide. When catalysis is over, the radical is transferred back to its resting position at Tyr_{122}; one tyrosyl radical can be active in a few hundred cycles. Although the two amino acid residues are more than 30 Å apart, they are connected by a single hydrogen-bonded chain, which is responsible for the conduction of the radical character. This hydrogen-bonded chain can be seen as composed of two different parts. One of them involves the metal centre in R2 and is formed by the Tyr_{122}, His_{118}, Asp_{237} and Trp_{48} residues (see Fig. 2). The other one consists of the path from Trp_{48}, which is still located in the vicinity of the iron dimer in R2, to Cys_{439}, at the active site in R1. The two amino acid residues immediately before Cys_{439} in the hydrogen-bonded chain are Tyr_{730} and Tyr_{731} (see Fig. 3); the other residues have not yet been identified because the structure of the protein in this region is not very clear, but apparently they include one more tyrosine residue, Tyr_{356}, which may be the one receiving the radical character from Trp_{48}.

Initially, the mechanism for the radical character relocation was suggested to consist of an electron transfer followed by local proton transfers to create neutral radicals. A theoretical study, carried on simple amino acid models (with vinyl alcohols as models for tyrosine residues), offered an alternative possibility, in which entire hydrogen atoms, protons and electrons, would be transferred in each step (Siegbahn et al. 1997). The hypothesis is termed hydrogen atom transfer (HAT), and although three different chemical mechanisms for this transfer were actually found in the study, all of them presented very small charge separation, which means that a hydrogen atom is indeed the entity being transferred.

A second theoretical study showed that the chemical environment around Tyr_{122} and Cys_{439}, does not favor a pure electron transfer mechanism between the two amino acid residues (Siegbahn et al. 1998a). In fact, the transfer was found to be endothermic by more than 40 kcal/mol, which makes it energetically unfeasible.

To gain insight into the details of the HAT mechanism for the radical transfer in RNR, Siegbahn et al. (1998b) undertook another theoretical study, in which the system was divided into two main subsets, according to the part of the hydrogen-bonded chain considered.

For the part of the chain closer to Cys_{439}, the radical transfer was suggested to occur in a sequence of individual steps of HAT between amino acid residues. Therefore, the study consisted of the evaluation of a HAT between the hydroxyl groups of two model tyrosines—both free and backbone linked—and between a tyrosine hydroxyl group and a thiol one. All these reactions were found to be energetically feasible, and presented predicted rates much faster than the overall turnover rate for RNR. Moreover, the charge separation was found to be very small, indicating a true HAT.

The radical transfer between Tyr_{122} and Trp_{48} over the iron dimer is considerably more complicated. It seems to involve a HAT as described previously—specifically from a water molecule, co-ordinated to one of the iron atoms, to the radical oxygen of Tyr_{122}—followed by a transfer of radical character through the His_{118}–Asp_{237}–Trp_{48} residue chain. Thus, the mechanism tested in the theoretical study corresponded essentially to a single step for the entire distance, the reactants being the resting state with a radical Tyr_{122} and a water molecule co-ordinated to the iron, and the products having the radical already placed in Trp_{48} and a normal hydroxyl group in Tyr_{122}. Since the step involves a large number of amino acid residues and the iron complex, a very approximate model was required. It consisted of one iron atom with its direct ligands—including the water molecule and a hydroxyl group modeling the oxo-bridge—and part of the side-chains of the hydrogen-bonded residues His_{118}, Asp_{237}, and Trp_{48}; Tyr_{122} was not included. After optimization of the reactants' and of the products' geometries, it was observed that the iron co-ordination and its spin were similar in both structures. In the products and as expected the spin population was mainly located at Trp_{48}.

Catalytic mechanism

Ribonucleotide reductase catalyzes the reduction of ribonuleotides to their corresponding deoyribonucleotides. Although apparently simple, this reaction has been shown to occur in a surprisingly complicated sequence of steps. A set of kinetic, spectroscopic, X-ray crystallographic, isotopic labeling and site-directed mutagenesis experiments has shed some light on the chemical events of the catalysis; the key amino acid residues involved were identified and a five-step hypothesis for the reaction mechanism was proposed. In the first step, the 3′-H atom is abstracted by the radical sulfur of Cys_{439}; this is followed by the transfer of a proton from the 3′-OH group to Glu_{441}, with concomitant protonation of the 2′-OH group by Cys_{225} and elimination of a water molecule; the third step corresponds to the abstraction of an H atom from the thiol group of Cys_{462} by the carbon C2′—directly or with mediation of the closer Cys_{225}; the resulting disulfide radical anion is subsequently reduced to a standard disulfide bond and a proton is transferred from Glu_{441} to the 3′-O atom, which replaces the charge in the glutamate residue and the spin density in the C3′ carbon; the final step consists of the donation of the H-atom by Cys_{439} back to that carbon; thus, the 2′-deoxyribonucleotide is formed and the essential tyrosyl radical is regenerated. Figure 7 illustrates the proposed mechanism.

In an effort to clarify the details of the mechanism by which class I RNRs dehydrate ribonucleotides, Siegbahn (1998) undertook a thorough theoretical study with small models of the substrate and of the main active site residues. The substrate was modeled with the sugar ring, the cysteines with methylthiol molecules, the glutamate with a formic acid, and the asparagine with formamide; neutral models were assumed to mimic the active site environment best. Computed activation energetics and geometries were compared in the same step for different residue permutations, and structures optimized in gas phase and in a continuum with a uniform dielectric constant of four. Consideration of multiple scenarios for each fundamental reaction step allowed for direct comparison of the plausibility of several mechanistic pathways. Overall, a six-step mechanism was proposed. The main differences between this proposal and the experimental one derive from the use of neutral models. Thus, in the second step, the protonation of the leaving hydroxyl group is not performed by the Cys_{225}, but by Glu_{441}, which is proposed to act as an acid–base catalyst, simultaneously abstracting the proton from the 3′-OH group and protonating the 2′-OH one. Moreover, the formation of the disulfide radical anion does not occur in the theoretical mechanism; instead, the oxidation of the two cysteines to a disulfide bond and the relocation of the spin in C3′ are proposed to take place through the intermediate formation of a C3′–S–Cys_{225} bond.

Theoretical calculations were again used (Himo and Siegbahn 2000) to identify the structure of a radical that had been detected in experimental studies with a mutant RNR (Persson et al. 1997). In the mutation experiments, the active site residue Glu_{441} was replaced by a glutamine residue; this resulted in the interruption of the substrate reaction at some stage and in the detection of two new transient, kinetically coupled radicals. The first radical was proposed latter to be a disulfide radical anion (Lawrence et al. 1999); the second was demonstrated to be substrate-derived but its position in the ribose ring remained elusive, the only really doubtful position being the C3′ carbon. Himo and Siegbahn (2000) compared the stability of three different ribose-derived radicals (namely the C1′, C2′ and C4′ radicals), and found the most stable to be the C4′ radical. Their calculations also led to some changes in the theoretically derived catalytic mechanism previously proposed by Siegbahn. In the new mechanism, the Cys_{225} sulfur does not add to the C3′ carbon of the ribose ring, but forms

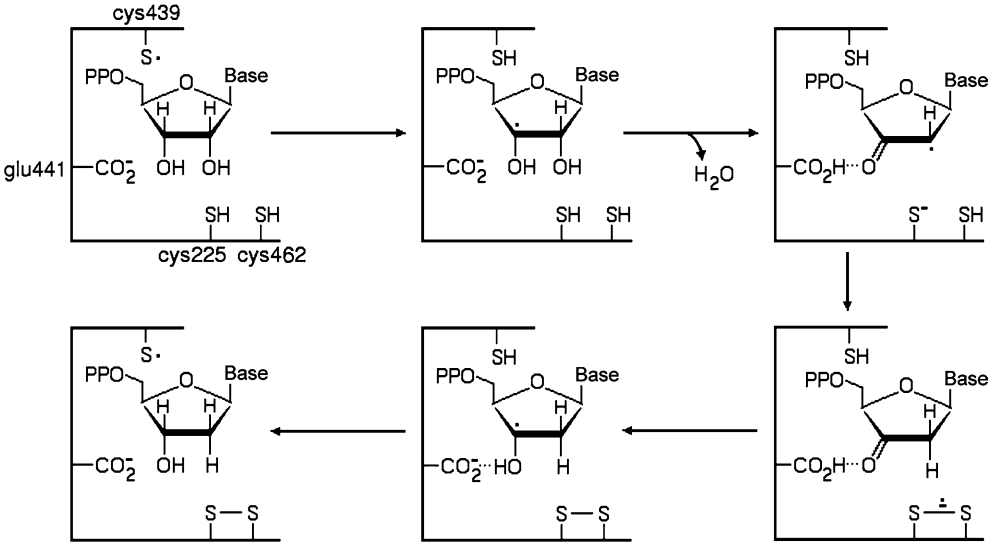

Fig. 7 The proposed catalytic mechanism of *E. coli* RNR

instead an earlier disulfide bond with the neighbor Cys_{462}.

The different proposals for the mechanism involved in the second step of RNR catalysis, that is, the elimination of the 2′-OH group from the ribose, were explored in another theoretical study (Fernandes et al. 2002). The models used were similar in size to Siegbahn's, but they were considered both in neutral and charged conditions. It was concluded that dehydration of the ribose may occur via two different acid or base catalyzed mechanisms. The first uses a protonated glutamate residue as a bifunctional catalyst, as proposed by Siegbahn; the second assumes that an unprotonated glutamate acts as a base, with a cysteine thiol group acting as an acidic catalyst. The latter should be the major pathway, given that at physiological pH only 0.2% of the glutamate residues will be protonated.

Pelmenschikov et al. (2004) reinvestigated the entire catalytic reaction pathway, with theoretical calculations. The active site residues were modeled by the same small molecules aforementioned, but with Glu_{441} being considered this time as anionic in the beginning of catalysis. As for the substrate, two alternative modeling schemes were applied, the smaller one consisting of the sugar ring with H-atoms replacing the 4′ and 1′ substituents, and the bigger including the diphosphate and the base groups explicitly; in the latter scheme both the terminal P-atom and an N-atom of the base were fixed; in both schemes the residues were also restrained in their flexibility by fixing one atom for each residue, according to the X-ray structure (Eriksson et al. 1997). The mechanistic pathway obtained with both modeling schemes is similar; it is also comparable overall to the first experiment-based proposal. The main difference is related with the proton transfer from the 3′-OH group to Glu_{441}: in this theoretical mechanism, the glutamate residue only stabilizes the transition state of step 2, by temporarily accepting the proton from the 3′-OH group, but remains anionic in the products of the reaction; the transfer of the proton only happens when the C2′ carbon receives the H-atom from a cysteine thiol, forming the ribose-derived furanone and the disulfide radical anion.

The detailed catalytic mechanism of RNR was also explored quantum-mechanically (by Cerqueira et al. 2004a). In the calculations, cysteine residues were modeled by methylthiol molecules, Glu_{441} by a formate anion, Asn_{437} by a formamide and the substrate by a ribose ring. The position of the residues was initially taken from the X-ray crystallographic structure (Uhlin and Eklund 1994), and although optimization of the structures was performed without any kind of restrictions, their position and orientation was retained, indicating that no strain is needed to build the active site. The mechanism scheme that resulted from this study is similar overall to the experimental proposal. One small difference is the role of Asn_{437} in the transfer of the radical character from the disulfide radical anion to the C3′ carbon (step 4); this residue had been proposed to be part of the transfer pathway, but the theoretical calculations indicate that its mediation is not required and suggest a direct radical character transfer from the disulfide to the nucleotide. Regarding the theoretical proposals, an important difference is the role of the water molecule after elimination from the C2′ carbon: while in the previous studies it was consistently kept in the active site and involved in hydrogen transfer reactions, here it was not included in the structures of the steps that follow its elimination, which seems reasonable given that water molecules can dissociate easily from the large, solvent-exposed RNR active site. Another difference particularly regarding Pelmenschikov's proposal, is that step 2 was found to involve the proton transfer from the 3′-OH group to Glu_{441}.

Another theoretical study undertook by Cerqueira et al. (2004b) was focused on the first step of RNR catalytic mechanism. In this work, a large model of the active site region that included a total of 130 atoms was used, instead of the small models of previous theoretical studies. Thus, it was possible to obtain a clearer insight into the role of the enzyme and particularly into the following aspects: enzyme–substrate interaction energies, specific transition state stabilization and substrate steric strain energies. It was concluded that the transition state of step 1 is stabilized in 4.0 kcal/mol by specific enzyme–substrate interactions, but this stabilization is cancelled by the cost in conformational energy for the enzyme to adopt the transition state geometry. It was found that the substrate binds RNR with almost no steric strain, which emphasizes the complementarity and specificity of the active site for nucleotide binding. The main role of the enzyme at the very beginning of the catalytic cycle was concluded to be the imposition of stereospecifity upon the substrate and to protect the enzyme radical from the solvent. The results also allowed the validation of the earlier results with the smaller models; at least in this step, the results obtained with both models are very close, indicating that the main contribution for the activation and reaction energies comes from the reacting part of the system.

Inhibition mechanism by substrate analogs

Ribonucleotide reductase substrate analogs are very important compounds from a clinical point of view. Their anti-cancer properties are well established, and one of them (Gemcitabine) is in clinical use since 1998; Tezacitabine is a similar compound, currently in Phase III clinical trials. Moreover, they are very interesting inhibitors to study theoretically since they are recognized by the active site as normal substrates and all the knowledge gathered around RNR normal catalysis can be applied in the study of their inhibition mechanisms. In fact, they are expected to react with the same amino acid residues of the active site, and surely the first reaction will occur with the radical Cys_{439}. The rest of the reaction pathway will be subsequently unravelled by exploring different possibilities, which should be both

chemically attractive and experimentally supported, and discarding the ones that present higher energetic landscapes.

Ribonucleotide reductase substrate analogs are usually modified in position C2′, which is the one that, in the natural catalysis, suffers reduction from 2′-OH to 2′-H. The interaction of these 2′-substituted substrate analogs with the RNR active site results in loss of the essential tyrosyl radical in R2 and/or covalent addition of a reaction intermediate to the enzyme in the R1 subunit. The 2′-chloro-2′-deoxynucleotides are an example of the former and 2′-azido-2′-deoxynucleotides of the latter. To gain insight into the underlying reasons for their different behavior, theoretical calculations were performed on the interaction of these two inhibitors with the main residues of the RNR active site (Fernandes and Ramos 2003a). Interestingly, it was observed that, in both cases, the initial abstraction of the 3′-H atom by the radical Cys_{439} is coupled with a proton transfer from the 3′-OH group to Glu_{441} and with the elimination of the 2′-substituent as an anion. After the decomposition of the inhibitor, the spin becomes localized in the carbon C2′, and two major pathways are possible: (1) C2′ receives an H-atom from Cys_{439}, the tyrosyl radical is regenerated and RNR will be inhibited by R1 alkylation or (2) C2′ receives the H-atom from Cys_{225} and the tyrosyl radical is lost. The X-ray crystallographic structure together with knowledge from catalytic mechanism, suggests that Cys_{225} would be the natural cysteine residue to perform the reaction. It was thus proposed that the first hypothesis only happens when the 2′-leaving group hinders the approach of Cys_{225} by forming a strong H-bond with it, which was observed to be the case with 2′-chloro-2′-deoxynucleotides. As for the 2′-azido-2′-deoxynucleotides, the addition of the azide group to the carbon C3′ after elimination from the C2′, opens the way for Cys_{225} to perform this reaction.

(*E*)-2′-fluoromethylene-2′-deoxycitidine-5′-diphosphate (FMCDP), also known as Tezacitabine, is an RNR substrate analog that possesses potent chemotherapeutic efficacy against several forms of cancer. It inhibits both RNR subunits, by destroying the essential tyrosyl radical in R2 and alkylating the active site in R1. EPR studies detected the formation of a new, inhibitor-derived radical, which accompanied the loss of the tyrosyl radical and involved covalent addition of an active-site residue. Based on these facts and in earlier mechanistic results for other 2′-substituted substrate analogs, a theoretical study was undertaken to explore all relevant chemical pathways that could be involved in the inhibition mechanism of FMCDP (Fernandes and Ramos 2003b). It was proposed that the major inhibition pathway would proceed through protonation of the fluorine atom by Cys_{439}, with subsequent elimination of fluoride and addition of the cysteine to the inhibitor. A final H-atom abstraction by Cys_{225} would place the spin density in the inhibitor, thus forming the radical detected in the experimental studies; the tyrosyl radical is destroyed by the covalent addition of Cys_{439} to the inhibitor, which simultaneously inactivates R1 by occluding the active site for further substrate binding.

A similar study was carried to explore the possible inhibition pathways of the 2′-azido-2′-deoxyribonucleotides substrate analogs (Pereira et al. 2004a). A set of experimental studies had indicated that inhibition of RNR involved loss of the tyrosyl radical and covalent modification of R1; the latter was exposed by the appearance of a characteristic absorbance at 320 nm, which was observed in other RNR mechanism-based inhibitions and is explained by the addition of a ribose-derived furanone to the enzyme. The formation of a new substrate-based transient radical concomitant with the destruction of the tyrosyl one was also detected, and an experiment-based mechanism was proposed, which had two possible endings corresponding to the formation of two different promising intermediate radical structures. The study led to the identification of the structure of the radical intermediate, between the two existing proposals; in this structure, the spin density is placed on one azide-derived nitrogen, which is bound to the sulfur atom of Cys_{225} and to the carbon C3′ of the inhibitor; the calculated Hypefine Coupling Constants for this radical were in excellent agreement with the correspondent experimental measurements. A new mechanistic pathway was also proposed, which was found to be the most energetically favoured; it led to the formation of the transient radical and subsequently to the production of the furanone responsible for R1 inactivation; the spin density is never replaced in Cys_{439}, which explains the loss of the tyrosyl radical. The identity of the radical, as well as the proposed pathway has been confirmed by later experimental findings (Fritscher et. al. 2005).

Gemcitabine (2′,2′-difluorodeoxycytidine) is a deoxycytidine analog that has shown promising results as an anti-cancer drug. Its use was approved by the FDA for the treatment of patients with non-small cell lung cancer, breast cancer and adenocarcinoma of the pancreas; in Europe it was approved additionally for the treatment of patients with bladder cancer. Moreover, it continues to be employed in multiple clinical trials to assess the benefit of different therapeutic approaches in those and in other types of cancer. Part of its activity involves inhibition of RNR, and some experimental studies aiming to gain insight into the details of this reaction observed that the absence or presence of reducing species in the medium influenced the enzyme subunit targeted; while the absence of reductants leads to loss of the essential tyrosyl radical in R2, with concomitant formation of a new nucleotide-based one, the availability of reducing species prevents the loss of the tyrosyl radical and results in R1 inhibition, probably by covalent modification; for either situation, no experiment-based mechanistic pathways were suggested. A theoretical study of the interaction of gemcitabine with the RNR active site was undertaken, which led to the first proposal of a mechanistic scheme for RNR inactivation in the absence of reductants (Pereira et al. 2004b); in this mechanism, the new nucleotide-based radical,

was proposed to be a C4′ radical, which had been previously suggested to be similar to the one detected in EPR experiments with a variant RNR (Persson et al. 1997; Himo and Siegbahn 2000).

The 2′-mercapto-2′-deoxyribonucleotides are yet another group of RNR substrate analogs with potential anti-cancer activity, whose inhibition mechanism was the subject of a theoretical study by Pereira et al. (2005). Experimentally, it had been found that RNR inhibition by these molecules only occurred in the presence of oxygen; in this situation, subunit R2 was specifically targeted with the destruction of the essential tyrosyl radical, and the role of R1 in RNR activity was not affected; the formation of a transient radical was also detected, which was proposed to be a perthiyl located in an active-site cysteine, probably Cys_{225}. If the experiment was carried out in anaerobic conditions, the enzyme remained active, the tyrosyl radical was not lost and the transient radical was not formed, suggesting that the reaction proceeded as with the normal substrate. Contrary to the other theoretical studies on inhibition mechanisms described so far in which small models were used to represent the active-site residues and the nucleotide (methylthiol for the cysteines, formate for Glu_{441} and the ribose-derived ring for the substrate), here the calculations were performed on a system containing ca. 130 atoms; it consisted of a cut-off of the R1 subunit, composed of a chain of seven amino acid residues (Ser_{436}–Asn_{437}–Leu_{438}–Cys_{439}–Leu_{440}–Glu_{441}–Ile_{442}) plus the side chain of Cys_{225}, and the same small model of the substrate. The results of the study were in agreement with the experimental mechanism by which RNR inhibition was proposed to take place when oxygen was available, and could refine and clarify such mechanistic proposal. The previously proposed structure for the transient radical detected in the presence of oxygen was also confirmed. Additionally, the first proposal was also made for the reaction pathway that occurs in anerobiosis and which does not affect RNR activity.

Conclusion

An overview of the main computational studies performed in the investigation of the action and inhibition mechanisms of the elusive enzyme RNR has been presented here. This kind of studies provides qualitative and quantitative insights that could not have been available from experiments alone. Thus, they are very useful as a complement to experimental studies, aiding in the validation or rebuttal of a given hypothesis. In fact, high accuracy quantum chemistry has become an indispensable tool for analyzing mechanisms of chemical reactions and, for small- and medium-sized systems, where the accuracy obtained is very high, mechanisms are now seldom accepted without support from theoretical calculations. One of the most useful aspects of quantum-chemical methods is that short-lived species are treated with equal ease and accuracy as long-lived ones, which means that it is possible to obtain structures and energies for transition states and unstable intermediates of chemical reactions, and also important information on radicals.

Ribonucleotide reductase is a medically very important enzyme, given that it is involved in the processes responsible for cell proliferation, and it is also a puzzling one, with a mechanism that took a lot of studies to unravel and involves radical generation by a metal cluster and complex radical reactions with the substrates. However, the deep understanding of such complex and intricate mechanisms is a fundamental prerequisite for the scientific and pharmaceutical rational drug design effort towards the development of more potent and efficient anti-cancer drugs. Computational methods aided in the understanding of the catalysis mechanism, and will continue to be useful in the investigation of the details that remain to be learned and that will help in finding new, more effective and safer ways of inhibiting the enzyme.

References

Balzarini J (2000) Effect of antimetabolite drugs of nucleotide metabolism on the anti-human immunodeficiency virus activity of nucleoside reverse transcriptase inhibitors. Pharmacol Ther 87:175–187

Bollinger JM Jr, Tong WH, Ravi N, Huynh BH, Edmonson DE, Stubbe J (1994) Mechanism of assembly of the tyrosyl radical-diiron(III) cofactor of *E. coli* ribonucleotide reductase. 2. Kinetics of the excess Fe^{2+} reaction by optical, EPR, and Mössbauer spectroscopies. J Am Chem Soc 116:8015–8023

Burdi D, Willems J-P, Riggs-Gelasco P, Antholine WE, Stubbe J, Hoffman BM (1998) The core structure of X generated in the assembly of the diiron cluster of ribonucleotide reductase: $^{17}O_2$ and $H_2^{17}O$ ENDOR. J Am Chem Soc 120:12910–12919

Cerqueira NMFSA, Femandes PA, Eriksson LA, Ramos MJ (2004a) New insights into a critical biological control step of the mechanism of Ribonucleotide reductase. J Mol Struct (Theochem) 709:53–65

Cerqueira NMFSA, Fernandes PA, Eriksson LA, Ramos MJ (2004b) Ribonucleotide activation by enzyme ribonucleotide reductase: understanding the role of the enzyme. J Comp Chem 25:2031–2037

Cerqueira NMFSA, Pereira S, Fernandes PA, Ramos MJ (2005) Overview of ribonucleotide reductase inhibitors: an appealing target in anti-tumour therapy. Curr Med Chem 12:1283–1294

Eriksson M, Uhlin U, Ramaswamy S, Ekberg M, Regnström K, Sjöberg B-M, Eklund H (1997) Binding of allosteric effectors to ribonucleotide reductase protein R1: reduction of active-site cysteines promotes substrate binding. Structure 5:1077–1092

Fernandes PA, Ramos MJ (2003a) Theoretical studies on the mode of inhibition of ribonucleotide reductase by 2'-substituted substrate analogues. Chem Eur J 9:5916–5925

Fernandes PA, Ramos MJ (2003b) Theoretical studies on the mechanism of inhibition of ribonucleotide reductase by (E)-2'-fluoromethylene-2'-deoxycitidine-5'-diphosphate. J Am Chem Soc 125:6311–6322

Fernandes PA, Eriksson LA, Ramos MJ (2002) The reduction of ribonucleotides catalyzed by the enzyme ribonucleotide reductase. Theor Chem Acc 108:352–364

Fritscher J, Artin E, Wnuk S, Bar B, Robblee JH, Kacprzak S, Kaupp M, Griffin RG, Bennati M, Stubbe J (2005) J Am Chem Soc, Article ASAP. DOI 10.1021/ja043111x

Han WG, Lovell T, Liu TQ, Noodleman L, (2003) A density functional evaluation of an Fe(III)-Fe(IV) model diiron cluster: Comparisons with ribonucleotide reductase intermediate X. Inorg Chem 42:2751–2758

Han WG, Lovell T, Liu TQ, Noodleman L (2004) Density functional study of a mu-1,1-carboxylate bridged Fe(III)-O-Fe(IV) model complex. 2. Comparison with ribonucleotide reductase intermediate X. Inorg Chem 43:613–621

Harrington JA, Spector T (1991) Human ribonucleotide reductase. Activation and inhibition by analogs of ATP. Biochem Pharmacol 42:759–763

Himo F, Siegbahn PEM (2000) Very stable ribonucleotide substrate radical relevant for class I ribonucleotide reductase. J Phys Chem B 104:7502–7509

Himo F, Siegbahn PEM (2003) Quantum chemical studies of radical-containing enzymes. Chem Rev 103:2421–2456

Ingram GM, Kinnaird JH (1999) Ribonucleotide reductase: a new target for antiparasite therapies. Parasitol Today 15:338–342

Johns DG, Gao WY (1998) Selective depletion of DNA precursors: an evolving strategy for potentiation of dideoxynucleoside activity against human immunodeficiency virus. Biochem Pharmacol 55:1551–1556

Kasrayan A, Persson AL, Sahlin M, Sjöberg B-M (2002) The conserved active site asparagine in class I ribonucleotide reductase is essential for catalysis. J Biol Chem 277:5749–5755

Lawrence CC, Obias H, Stubbe J, Bennati M, Bar G, Grifin RG (1999) High-field EPR detection of a disulfide radical anion in the reduction of cytidine 5'-diphosphate by the E441Q R1 mutant of Escherichia coli ribonucleotide reductase. Proc Natl Acad Sci USA 96:8979–8984

Logan DT, Su X-D, Åberg A, Regnström K, Hadju J, Eklund H, Nordlund P (1996) Crystal structure of reduced protein R2 of ribonucleotide reductase: the structural basis for oxygen activation at a dinuclear iron site. Structure 4:1053–1064

Manegold C (2004) Gemcitabine (Gemzar) in non-small cell lung cancer. Expert Rev Anticancer Ther 4:345–360

Noodleman L, Lovell T, Han WG, Li J, Himo F. (2004) Quantum chemical studies of intermediates and reaction pathways in selected enzymes and catalytic synthetic systems. Chem Rev 104:459–508

Nordlund P, Sjöberg B-M, Eklund H (1990) 3-Dimensional structure of the free radical protein of ribonucleotide reductase. Nature 345:593–598

Nordlund P, Eklund H (1993) Structure and function of the *Escherichia coli* ribonucleotide reductase protein R2. J Mol Biol 232:123

Pelmenschikov V, Cho KB, Siegbahn PEM (2004) Class I ribonucleotide reductase revisited: the effect of removing a proton on Glu441. J Comp Chem 25:311–321

Pereira S, Fernandes PA, Ramos MJ (2004a) Theoretical study of ribonucleotide reductase mechanism-based inhibition by 2'-azido-2'-deoxyribonucleoside-5'-diphosphates. J Comp Chem 25:227–237

Pereira S, Fernandes PA, Ramos MJ (2004b) Mechanism for ribonucleotide reductase inactivation by the anticancer drug gemcitabine. J Comp Chem 25:1286–1294

Pereira S, Fernandes PA, Ramos MJ (2005) Theoretical study on the inhibition of ribonucleotide reductase by 2'-mercapto-2'-deoxyribonucleoside-5'-diphosphates. J Am Chem Soc 127:5174–5179

Persson AL, Eriksson M, Katterle B, Pötsh S, Sahlin M, Sjöberg B-M (1997) A new mechanism-based radical intermediate in a mutant R1 protein affecting the catalytically essential Glu441 in *Escherichia coli* ribonucleotide reductase. J Biol Chem 272:31533–31541

Reichard P (1993) From RNA to DNA, why so many ribonucleotide reductases? Science 260:1773–1777

Romanelli F, Pomeroy C, Smith KM (1999) Hydroxyurea to inhibit human immunodeficiency virus-1 replication. Pharmacotherapy 19:196–204

Siegbahn PEM (1998) Theoretical study of the substrate mechanism of ribonuleotide reductase. J Am Chem Soc 120:8417–8429

Siegbahn PEM (1999) Theoretical model studies of the iron dimer complex of MMO and RNR. Inorg Chem 38:2880–2889

Siegbahn PEM, Blomberg MRA, Crabtree RH (1997) Hydrogen transfer in the presence of amino acid radicals. Theor Chem Acc 97:289–300

Siegbahn PEM, Blomberg MRA, Pavlov M (1998a) A comparison of electron transfer in ribonucleotide reductase and the bacterial photosynthetic reaction center. Chem Phys Lett 292:421–430

Siegbahn PEM, Eriksson L, Himo F, Pavlov M (1998b) Hydrogen atom transfer in ribonucleotide reductase (RNR). J Phys Chem B 102:10622–10629

Stubbe J, van Der Donk WA (1998) Protein radicals in enzyme catalysis. Chem Rev 98:705–762

Sturgeon BE, Burdi D, Chen S, Huynh B-H, Edmondson DE, Stubbe J, Hoffman BM (1996) Reconsideration of X, the diiron intermediate formed during cofactor assembly in *E. coli* ribonucleotide reductase. J Am Chem Soc 118:7551–7557

Torrent M, Musaev DG, Morokuma K (2001) The flexibility of carboxylate ligands in methane monooxygenase and ribonucleotide reductase: a density functional study. J Phys Chem B 105:322–327

Torrent M, Musaev DG, Basch H, Morokuma K (2002) Computational studies of reaction mechanisms of methane monooxygenase and ribonucleotide reductase. J Comp Chem 23:59–76

Tripathy D. (2002) Gemcitabine in breast cancer: future directions. Clin Breast Cancer 3:45–48

Tsimberidou AM, Alvarado Y, Giles FJ (2002) Evolving role of ribonucleoside reductase inhibitors in hematologic malignancies. Expert Rev Anticancer Ther 2:437–448

Uhlin U, Eklund H (1994) Structure of ribonucleotide reductase protein R1. Nature 370:533–539

Wei PP, Skulan AJ, Mitic N, Yang YS, Saleh L, Bollinger JM, Solomon EI (2004) Electronic and spectroscopic studies of the non-heme reduced binuclear iron sites of two ribonucleotide reductase variants: comparison to reduced methane monooxygenase and contributions to O_2 reactivity. J Am Chem Soc 126:3777–3788

Yang Y-S, Baldwin J, Ley BA, Bollinger JM Jr, Solomon EI (2000) Spectroscopic and electronic structure description of the reduced binuclear non-heme iron active site in ribonucleotide reductase from *E. coli*: comparison to reduced Δ^9 desaturase and electronic structure contributions to differences in O_2 reactivity. J Am Chem Soc 122:8495–8510